Journal of Magnetic Resonance **139,** 302–307 (1999)
Article ID jmre.1999.1776, available online at http://www.idealibrary.com on IDEAL®

Selection Rules for Multiple Quantum NMR Excitation in Solids: Derivation from Time-Reversal Symmetry and Comparison with Simulations and ^{13}C NMR Experiments

Robert Tycko[1]

Laboratory of Chemical Physics, National Institute of Diabetes and Digestive and Kidney Diseases, National Institutes of Health, Building 5, Room 112, Bethesda, Maryland 20892-0520

Received December 7, 1998; revised March 31, 1999

New derivations of selection rules for excitation and detection of multiple quantum coherences in coupled spin-1/2 systems are presented. The selection rules apply to experiments in which the effective coupling Hamiltonian used for multiple quantum excitation is both time-reversal invariant and time-reversible by a phase shift of the radiofrequency pulse sequence that generates the effective couplings. The selection rules are shown to be consequences of time-reversal invariance and time-reversibility and otherwise independent of the specific form of the effective coupling Hamiltonian. Numerical simulations of multiple quantum NMR signal amplitudes and experimental multiple quantum excitation spectra are presented for the case of a multiply ^{13}C-labeled helical polypeptide. The simulations and experiments confirm the selection rules and demonstrate their impact on multiple quantum ^{13}C NMR spectra in this biochemically relevant case.

Key Words: **multiple quantum NMR; time-reversal; NMR theory; solid state NMR; peptides.**

INTRODUCTION

Multiple pulse, multiple quantum (MQ) nuclear magnetic resonance (NMR) spectroscopy of solids, originally demonstrated by Yen and Pines (*1*), has developed into a useful tool for estimating the number of nuclear spins in a coupled system (*2–5*). MQ "spin counting" of protons and ^{19}F nuclei can provide important structural information about inorganic (*6–9*) and organic (*10–14*) materials of technological interest. In addition, MQ NMR spectroscopy has been the basis for fundamental studies of the quantum dynamics of many-spin systems in solids (*15–20*). Recently, we demonstrated the feasibility of high-order MQ excitation in dilutely ^{13}C-labeled organic compounds (*21*). ^{13}C MQ NMR spectroscopy may prove to be a useful probe of the conformations and oligomerization states of ^{13}C-labeled biopolymers such as peptides and proteins.

An important aspect of MQ spectroscopy of solids is the use of multiple pulse sequences to create effective dipole–dipole coupling Hamiltonians that are time-reversible, i.e., that can be reversed in sign by some experimental manipulation such as a shift of the phase of the radiofrequency (RF) pulses (*1, 2, 5, 15, 22*). The property of time-reversibility is logically distinct from the property of time-reversal invariance (*23*). The latter property is shared by all effective Hamiltonians that are bilinear or even-power functions of spin angular momentum operators, while the former property obtains only in special cases. When the effective coupling Hamiltonian in the preparation period of the MQ experiment is opposite in sign to the effective coupling Hamiltonian in the mixing period of the experiment, all MQ transitions contribute to the MQ spectrum with the same phase (*1, 2, 22, 24*). Destructive interference among unresolved MQ transitions, which would otherwise drastically reduce the MQ signal amplitude (*1, 22, 24*), is thereby eliminated.

To date, two forms of time-reversible effective couplings have been employed in MQ NMR experiments in solids. One is a double quantum Hamiltonian (*1, 2, 15, 22*) of the form

$$H_{\mathrm{DQ}} = \sum_{i>j} d_{ij}(I_{yi}I_{yj} - I_{xi}I_{xj}), \qquad [1]$$

where $\mathbf{I}_i$ and $\mathbf{I}_j$ are the spin angular momentum vector operators for spins i and j and d_{ij} is the coupling constant. The other is a single quantum Hamiltonian (*5*) of the form

$$H_{\mathrm{SQ}} = \sum_{i>j} d_{ij}(I_{zi}I_{xj} + I_{xi}I_{zj}). \qquad [2]$$

The sign of H_{DQ} is reversed by a $\pi/2$ phase shift of all RF pulses in the multiple pulse sequence used to generate H_{DQ}, which has the effect of rotating H_{DQ} by $\pi/2$ about z in angular momentum space. The sign of H_{SQ} is reversed by a π phase shift (or alternatively by application of π_x pulses at the beginning and end of the multiple pulse sequence). Use of Hamiltonians H_{DQ} and H_{SQ} leads to particular selection rules that govern the possible orders and ranks (defined below) of MQ

[1] Fax: 301-496-0825, E-mail: tycko@helix.nih.gov.

1090-7807/99

coherences that may be excited and detected in MQ spectra when the nuclear spin system is initially at thermal equilibrium in a strong magnetic field. The selection rules are particularly important in spin counting applications when the number of coupled spins N is relatively small, because the selection rules may prohibit excitation of the highest-order MQ transition (i.e., the N-quantum transition in a system of coupled spin-1/2 nuclei) for some values of N. In previous publications (*5*, *15*), the selection rules were derived by analysis of the Liouville–von Neumann equation $\dot{\rho}(t) = i[\rho(t), H]$, using the well-known commutation relations among spin angular momentum operators and the explicit forms for H given in Eqs. [1] and [2]. An implicit assumption in these derivations is that the spin density operator $\rho(t)$ at any time t can be derived from $\rho(0)$ by iterative evaluation of commutators, as in the series expansion

$$\rho(t) = \rho(0) + it[\rho(0), H] - \frac{t^2}{2}[[\rho(0), H], H] - i\frac{t^3}{6}[[[\rho(0), H], H], H] + \ldots . \quad [3]$$

The initial condition $\rho(0)$ is proportional to

$$I_z = \sum_i I_{zi} \quad [4]$$

for longitudinal spin polarization, as in thermal equilibrium with a static magnetic field along z, or to a linear combination of I_x and I_y for transverse magnetization.

This paper presents alternative derivations of the selection rules for excitation and detection of MQ coherences in systems of spin-1/2 nuclei with effective coupling Hamiltonians that are time-reversible under an rf phase shift, as in Eqs. [1] and [2]. The derivations given below do not depend on any series expansions or commutation relations, and are therefore independent of perturbation theory and of any conceivable concerns (*16*) regarding the convergence of Eq. [3]. Instead, these derivations makes use of the time-reversal invariance and time-reversibility of the effective Hamiltonian. This paper also presents the results of numerical simulations of MQ excitation spectra that confirm the selection rules and are relevant to possible MQ NMR measurements on ^{13}C-labeled peptides and proteins. Finally, experimental MQ NMR excitation spectra of a ^{13}C-labeled, 20-residue peptide, in lyophilized solid form, are presented and briefly discussed.

THEORY

The nuclear spin density operator $\rho(t) = e^{-iHt}\rho(0)e^{iHt}$, which describes the state of the system of N coupled spins after evolution for time t under the time-independent effective Hamiltonian H, can in general be expressed as a linear combination of Lth-rank (or L-spin), M-quantum operators $A_{L,M,q}$. Each $A_{L,M,q}$ is a product of L angular momentum operators I_{zi}, $I_{+,i}$, or $I_{-,i}$, with M equal to the difference between the number of raising operators $I_{+,i}$ and the number of lowering operators $I_{-,i}$ in the product. The index q is required to distinguish the various operators with the same L and M from one another. For example, $I_{z1}I_{+,3}I_{-,4}I_{+,6}I_{+,7}I_{z9}$ is one possible $A_{6,2,q}$ operator in a spin system with $N \geq 9$. For coupled spin-1/2 systems, the $A_{L,M,q}$ operators can be defined in such a way that no more than one of the operators I_{zi}, $I_{+,i}$, or $I_{-,i}$ appears in the product for each spin i. To within a normalization constant, the amplitude of the $A_{L,M,q}$ component in $\rho(t)$, i.e., the probability amplitude for exciting the qth Lth-rank, M-quantum coherence, is given by

$$\mathcal{A}_{L,M,q}(t) = \mathrm{Tr}\{A^\dagger_{L,M,q}e^{-iHt}\rho(0)e^{iHt}\}. \quad [5]$$

The selection rules specify the values of L and M for which $\mathcal{A}_{L,M,q}(t)$ is not necessarily zero.

The following derivations of MQ selection rules make use of the antilinear, antiunitary time-reversal operator K (*23*), which has the properties $K\mathbf{I}K^{-1} = -\mathbf{I}$, $K(i)K^{-1} = -i$, and $\mathrm{Tr}\{KBK^{-1}\} = \mathrm{Tr}\{B\}^*$. The last property follows from $\langle a|(K|b\rangle) = [(\langle b|K)|a\rangle]^*$, where $|a\rangle$ and $|b\rangle$ are arbitrary kets, and $K^\dagger = K^{-1}$. For coupled spin-1/2 systems, $KA_{L,M,q}K^{-1} = (-1)^L A^\dagger_{L,M,q}$. The derivations also make use of several well-known properties of linear operators and their traces: (1) $(BC)^\dagger = C^\dagger B^\dagger$, which holds for any linear operators B and C; (2) $\mathrm{Tr}\{BC\} = \mathrm{Tr}\{CB\}$; (3) $\mathrm{Tr}\{RBR^{-1}\} = \mathrm{Tr}\{B\}$, which holds for any linear operator R with an inverse R^{-1}; and (3) $\mathrm{Tr}\{B^\dagger\} = \mathrm{Tr}\{B\}^*$. In addition, the derivations assume that $R_z(\phi_{\mathrm{TR}})HR_z(\phi_{\mathrm{TR}})^{-1} = -H$, where $R_z(\phi_{\mathrm{TR}})$ is the operator for a rotation of all spin angular momenta about z by ϕ_{TR} (i.e., an RF phase shift ϕ_{TR} reverses the sign of H), and $KHK^{-1} = H$ (i.e., H is time-reversal invariant). Note that $R_z(\phi_{\mathrm{TR}})A_{L,M,q}R_z(\phi_{\mathrm{TR}})^{-1} = e^{-iM\phi_{\mathrm{TR}}}A_{L,M,q}$.

Consider first the initial condition $\rho(0) = I_z$. Then

$$\begin{aligned}
\mathcal{A}_{L,M,q}(t) &= \mathrm{Tr}\{(A^\dagger_{L,M,q}e^{-iHt}I_z e^{iHt})^\dagger\}^* && [6a]\\
&= \mathrm{Tr}\{A_{L,M,q}e^{-iHt}I_z e^{iHt}\}^* && [6b]\\
&= \mathrm{Tr}\{K(A_{L,M,q}e^{-iHt}I_z e^{iHt})K^{-1}\} && [6c]\\
&= (-1)^{L+1}\mathrm{Tr}\{A^\dagger_{L,M,q}e^{iHt}I_z e^{-iHt}\} && [6d]\\
&= (-1)^{L+1}\mathrm{Tr}\{R_z(\phi_{\mathrm{TR}})A^\dagger_{L,M,q}e^{iHt}I_z e^{-iHt}R_z(\phi_{\mathrm{TR}})^{-1}\} && [6e]\\
&= (-1)^{L+1}e^{iM\phi_{\mathrm{TR}}}\mathrm{Tr}\{A^\dagger_{L,M,q}e^{-iHt}I_z e^{iHt}\} && [6f]\\
&= (-1)^{L+1}e^{iM\phi_{\mathrm{TR}}}\mathcal{A}_{L,M,q}(t). && [6g]
\end{aligned}$$

Therefore, $\mathcal{A}_{L,M,q}(t)$ can be nonzero only if

$$(-1)^{L+1}e^{iM\phi_{\mathrm{TR}}} = 1. \quad [7]$$

If $\phi_{TR} = \pi/2$, as in the case $H = H_{DQ}$, this implies the selection rules that M be an even integer and that $L + M/2$ be an odd integer. If $\phi_{TR} = \pi$, as in the case $H = H_{SQ}$, this implies the selection rule that $L + M$ be an odd integer.

In a system of N spin-1/2 nuclei, the N-quantum coherence has $L = M = N$. It is impossible to excite the N-quantum coherence from an initial condition $\rho(0) = I_z$ in a spin-1/2 system when $\phi_{TR} = \pi$. When $\phi_{TR} = \pi/2$, the N-quantum coherence can be excited from an initial condition $\rho(0) = I_z$ only if N is an odd multiple of two.

For the initial condition $\rho(0) = I_x$, the same argument leads to

$$\mathcal{A}_{L,M,q}(t) = (-1)^{L+1} e^{iM\phi_{TR}} [\cos\phi_{TR} Tr\{(A^{\dagger}_{L,M,q} e^{-iHt} I_x e^{iHt})^{\dagger}\} + \sin\phi_{TR} \mathrm{Tr}\{(A^{\dagger}_{L,M,q} e^{-iHt} I_y e^{iHt})^{\dagger}\}]. \quad [8]$$

If $\phi_{TR} = \pi$, Eq. [8] implies the selection rule that $L + M$ be an even integer. Excitation of the N-quantum coherence in a system of N spin-1/2 nuclei is allowed, in general. Equation [8] does not restrict L and M if $\phi_{TR} = \pi/2$, but the selection rule that M be an odd integer in this case follows simply from

$$\mathcal{A}_{L,M,q}(t) = \mathrm{Tr}\{R_z(\pi) A^{\dagger}_{L,M,q} e^{-iHt} I_x e^{iHt} R_z(\pi)^{-1}\} \quad [9a]$$

$$= -e^{iM\pi} \mathrm{Tr}\{A^{\dagger}_{L,M,q} e^{-iHt} I_x e^{iHt}\}. \quad [9b]$$

Selection rules for $\rho(0) = I_y$ are identical to those for $\rho(0) = I_x$.

Note that the derivations given above depend on ϕ_{TR} but not on other details of H. The selection rules therefore apply to forms of effective couplings more general than those in Eqs. [1] and [2]. However, the selection rules apply only to spin-1/2 systems. In non-spin-1/2 systems, the simplest general form for the operators $A_{L,M,q}$ is a product of terms $I_{zi}^{m_i} I_{+,i}^{n_i}$ or $I_{zi}^{m_i} I_{-,i}^{n_i}$ with $m_i, n_i \geq 0$. Unless $m_i + n_i \leq 1$ for all i, $KA_{L,M,q}K^{-1} \neq (-1)^L A^{\dagger}_{L,M,q}$ in general. Previous derivations of MQ selection rules (*5*, *15*) presumably also apply only to spin-1/2 systems, although this is not explicitly stated.

When the Hermitian detected operator D in a MQ NMR experiment is the same as the initial condition, as is usually the case (*1–5*, *21*, *22*, *24*), the selection rules for excitation and detection of MQ coherences are identical. The probability amplitude for detecting the coherence $A_{L,M,q}$ after evolution under the time-reversed Hamiltonian during the mixing period of duration t is given by

$$\mathcal{B}_{L,M,q}(t) = \mathrm{Tr}\{D e^{iHt} A_{L,M,q} e^{-iHt}\}. \quad [10]$$

It follows that $\mathcal{B}_{L,M,q}(t) = \mathcal{A}_{L,M,q}(t)^*$ when $D = \rho(0)$.

SIMULATIONS

Numerical simulations of multiple-quantum excitation under time-reversible Hamiltonians H_{SQ} and H_{DQ} were carried out for a polyalanine peptide in an ideal α-helical conformation. The simulations assume that the peptide is labeled with ^{13}C at the methyl side chain positions of four, five, or six alanine residues, separated by two unlabeled residues (e.g., residues i, $i + 3$, $i + 6$, $i + 9$, $i + 12$, and $i + 15$ in the case of six ^{13}C labels). The coordinates of the methyl carbons in the α-helical conformation were determined with the QUANTA modeling program (Molecular Simulations, Inc.), using standard bond lengths and angles, and backbone dihedral angles $(\phi, \psi, \omega) = (-57°, -47°, 180°)$. With this geometry, the shortest distances between methyl labels are $r_{min} = 5.8$ Å. The maximum dipole–dipole coupling constant $\gamma^2\hbar/2\pi r_{min}^3$ is 39 Hz, where γ is the magnetogyric ratio. This is the maximum value of $d_{ij}/2\pi$ in Eqs. [1] and [2]. Placement of ^{13}C labels at every third residue was chosen for these simulations because this labeling scheme may allow the differentiation of a helical conformation, which brings the labels relatively close together, from an extended conformation, which leads to significantly longer internuclear distances and weaker couplings, in ^{13}C MQ NMR experiments on real peptides or proteins.

The multiple pulse sequence $[-\tau'/2\text{–}90_x\text{–}\tau\text{–}90_x\text{–}\tau'\text{–}90_x\text{–}\tau\text{–}90_x\text{–}\tau'\text{–}90_{-x}\text{–}\tau\text{–}90_{-x}\text{–}\tau'\text{–}90_{-x}\text{–}\tau\text{–}90_{-x}\text{–}\tau'/2\text{–}]_n$ was used to generate the effective coupling Hamiltonian H_{DQ} in the simulations (*1*, *2*, *22*). The sequence $45_y\text{–}[-\tau/2\text{–}90_x\text{–}\tau'\text{–}90_x\text{–}\tau\text{–}90_x\text{–}\tau'\text{–}90_x\text{–}\tau\text{–}90_{-x}\text{–}\tau'\text{–}90_{-x}\text{–}\tau\text{–}90_{-x}\text{–}\tau'\text{–}90_{-x}\text{–}\tau/2\text{–}]_n\text{–}45_{-y}$ was used to generate H_{SQ} (*5*). In both cases, $\tau = 798$ μs and $\tau' = 397$ μs. The 90° and 45° pulse lengths were 4 and 2 μs, respectively. The integer n indicates the number of repetitions of the multiple pulse cycle in the MQ preparation period and in the mixing period of a simulated experiment, so that the lengths of the preparation and mixing periods would be $4.812 \times n$ ms. The evolution operator $U(n)$ and the density operator $\rho(n) \equiv U(n)\rho(0)U(n)^{-1}$ were calculated as $2^N \times 2^N$ matrices, using a direct-product basis for the system of N spin-1/2 nuclei. The total M-quantum signal amplitude $S_M(n)$ (i.e., the probability amplitude for excitation of an M-quantum coherence at the end of the preparation period and detection of signals from this coherence at the end of the mixing period, summed over all M-quantum coherences) was then evaluated as $S_M(n) = \Sigma'_{a,b} |\langle b|\rho(n)|a\rangle|^2$, where $\Sigma'_{a,b}$ indicates a sum over all pairs of direct-product states $|a\rangle$ and $|b\rangle$ that satisfy $|\langle b|I_z|b\rangle - \langle a|I_z|a\rangle| = M$. Finally, $S_M(n)$ values calculated for 256 directions of the external magnetic field relative to a molecule-fixed axis system were summed and normalized to yield the powder-average M-quantum signal amplitudes $\mathcal{S}_M(n)$.

The results of calculations for $N = 4$, 5, 6 and $n = 1$, 2, 4, 8 are displayed in Fig. 1 for $\rho(0) = I_z$ and in Fig. 2 for $\rho(0) = I_x$. The numerical results are in full agreement with the selection rules discussed above. In particular, using H_{DQ}, $\mathcal{S}_M(n)$ is nonzero only for even values of M when $\rho(0) = I_z$ and odd values of M when $\rho(0) = I_x$. For the four-spin system with $\rho(0) = I_z$, $\mathcal{S}_4(n)$ is zero to within the precision of the calculations for all values of n. For the six-spin system with

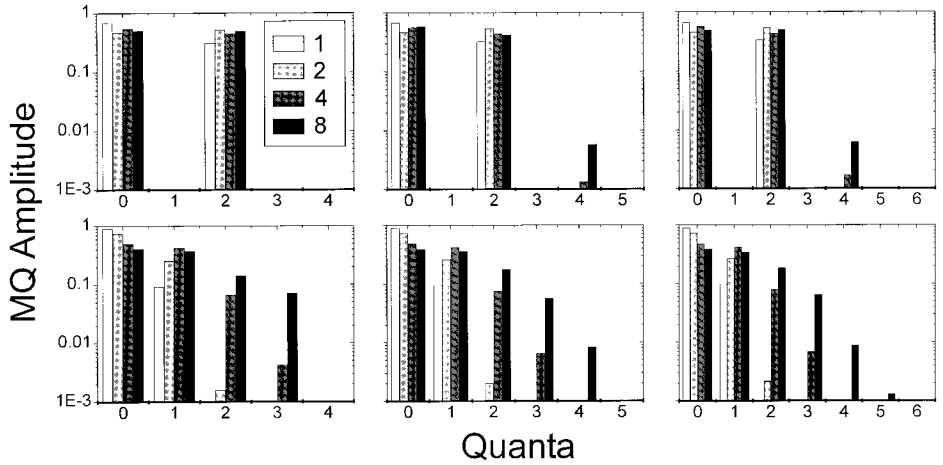

FIG. 1. Simulated multiple quantum ^{13}C NMR signal amplitudes for an α-helical polyalanine peptide with ^{13}C labels at methyl carbon positions of every third alanine residue. The number of labels is 4 (left), 5 (middle), or 6 (right). The effective dipole–dipole coupling Hamiltonian is H_{DQ} (top) or H_{SQ} (bottom). The initial condition is $\rho(0) = I_z$. Results are shown for $n = 1$, 2, 4, and 8, corresponding to multiple quantum preparation and mixing periods of 4.812, 9.624, 19.248, and 38.496 ms. Note that the signal amplitudes are plotted on a logarithmic scale.

$\rho(0) = I_z$, $\mathcal{I}_6(n)$ is small but nonzero. For example, $\mathcal{I}_6(8) = 0.000084$. Using H_{SQ}, $\mathcal{I}_M(n)$ is zero to within the precision of the calculations for $M = N$ when $\rho(0) = I_z$. All values of $\mathcal{I}_M(n)$ are nonzero for large n when $\rho(0) = I_x$.

EXPERIMENTAL MULTIPLE QUANTUM EXCITATION SPECTRA

Experiments were carried out on the 20-residue peptide helix20 (sequence Ac–TyrAlaGluAlaAlaAlaLysAlaGluAlaAlaAlaLysAlaGluAlaAlaAlaLysLys–NH_2, where Ac and NH_2 represent acetyl and amide capping groups at the N- and the C-terminus), synthesized by standard solid-phase methods with ^{13}C labels at the methyl carbons of Ala5, Ala8, Ala11, Ala14, and Ala17. This peptide was designed to be highly α-helical. A theoretical analysis of the helix20 sequence, using the AGADIR program (*25*), predicts helix contents greater than 75% from Ala4 through Ala18 at pH 7.0, 274 K, and zero ionic strength. Circular dichroism measurements on helix20 in aqueous solution (9 μM peptide concentration, 5 mM phosphate buffer, pH 6.8, 274 K) reveal minima in the molar ellipticity $[\theta]$ at 222 and 208 nm wavelengths, characteristic of an α-helical conformation. The observed value $[\theta]_{222} = -14.7 \times 10^3$ deg-cm^2/dmol suggests an average helix content of approximately 50%.

Figure 3 shows experimental MQ NMR excitation spectra of a 30 mg sample of ^{13}C-labeled helix20 in lyophilized solid form, obtained at 9.39 T (100.8 MHz ^{13}C NMR frequency) using a Chemagnetics Infinity-400 spectrometer with a home-built static double-resonance probe. The relatively low solubility of helix20 precluded experiments on frozen solutions.

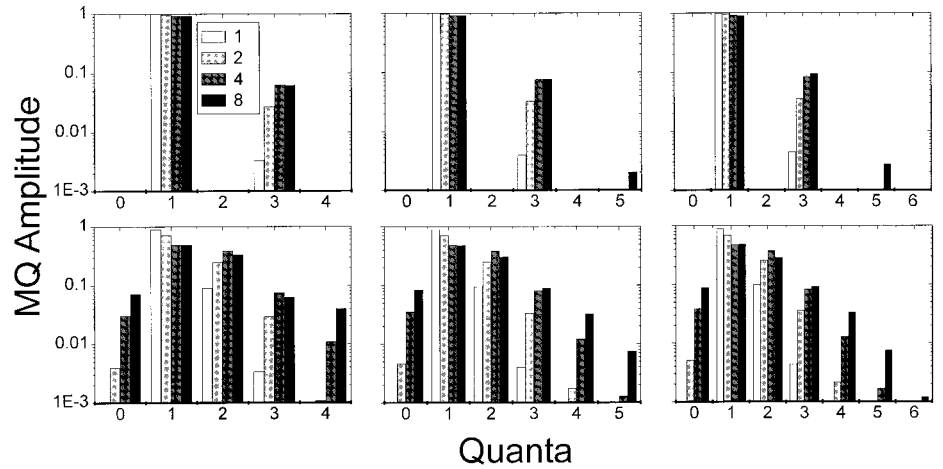

FIG. 2. Same as Fig. 1, but with the initial condition $\rho(0) = I_x$.

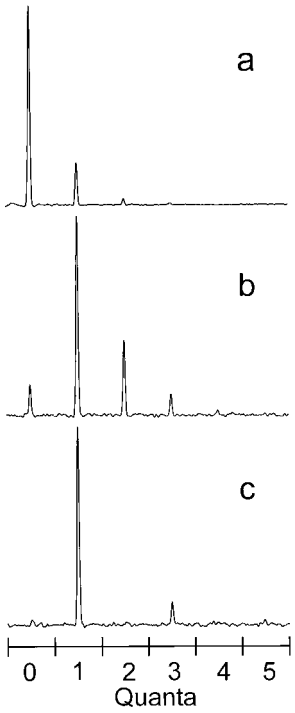

FIG. 3. Experimental ^{13}C multiple quantum NMR spectra of the 20-residue peptide helix20, with ^{13}C labels at methyl carbons of Ala5, Ala8, Ala11, Ala14, and Ala17, in lyophilized form. The effective dipole–dipole coupling Hamiltonian for multiple quantum excitation is the single quantum operator H_{SQ} in (a) and (b), and the double quantum operator H_{DQ} in (c). The initial condition and detected operator are I_z in (a) and I_x in (b) and (c). Excitation spectra for multiple quantum orders 0 through 5 are plotted side-by-side, with a spectral width of 50 kHz in each order. See the text for experimental conditions.

The experiments were carried out and the data were analyzed as previously described (*21*), but with the addition of TPPM decoupling (*26*) during the MQ preparation and mixing periods and with the use of the multiple pulse sequence of Suter *et al.* (*5*), modified by insertion of π pulses to remove effects of chemical shift anisotropy (*21*), to create a single quantum effective ^{13}C–^{13}C dipole–dipole coupling Hamiltonian for Figs. 3a and 3b. The initial condition and detected operator were selected by optional $\pi/2$ pulses at the beginning of the MQ preparation period and the end of the MQ mixing period. Spectra in Fig. 3 were obtained with MQ preparation and mixing periods of 19.2 ms. ^{13}C RF pulse amplitudes were 36 kHz during MQ preparation and mixing. The ^{1}H decoupling amplitude was 85 kHz. A total of 8192 scans were acquired for Figs. 3a and 3b, and 2048 scans for Fig. 3c.

In Fig. 3a, the initial condition and detected operator are both I_z and the effective coupling Hamiltonian is H_{SQ}. In Fig. 3b, the initial condition and detected operator are both I_x and the effective coupling Hamiltonian is H_{SQ}. In Fig. 3c, the initial condition and detected operator are both I_x and the effective coupling Hamiltonian is H_{DQ}. The signal intensities in the various MQ orders are consistent with the selection rules discussed above. The signal intensities are in approximate agreement with the simulations in Figs. 1 and 2, with the assumption that approximately 70% of the total signal intensity arises from peptides in an α-helical conformation and the remaining signal intensity arises from relatively isolated ^{13}C nuclei, perhaps in molecules with a more extended conformation. Intermolecular dipole–dipole couplings may also play a role in the excitation of MQ coherences. In particular, the enhancement of the three- and four-quantum signals in Fig. 3b, when compared with the simulations in Fig. 2, may be due to intermolecular couplings.

The MQ excitation spectra in Fig. 3 should be viewed as preliminary results in light of the uncertainties described above regarding the conformational distribution of helix20 in lyophilized form and the role of intermolecular couplings. Nonetheless, these spectra demonstrate the feasibility of MQ NMR measurements on multiply ^{13}C-labeled biopolymers and the influence of the MQ selection rules on the experimental spectra.

CONCLUSION

Selection rules for MQ NMR excitation in coupled spin-1/2 systems with time-reversible and time-reversal invariant effective coupling Hamiltonians are derived above in a way that does not depend on the explicit form of the effective Hamiltonians, commutation relations, or series expansions. The selection rules are therefore shown to be direct consequences of time-reversibility and time-reversal invariance. The numerical simulations on coupled ^{13}C spin systems illustrate the impact of the selection rules on MQ excitation spectra in a case that is of relevance to MQ NMR experiments on ^{13}C-labeled polypeptides. The feasibility of using ^{13}C MQ NMR measurements to investigate peptide and protein conformations, in particular helical secondary structure and helix–coil transitions, is suggested by the experimental MQ NMR excitation spectra of the multiply ^{13}C-labeled helix20 peptide.

REFERENCES

1. Y. S. Yen and A. Pines, Multiple quantum NMR in solids, *J. Chem. Phys.* **78,** 3579–3582 (1983).
2. J. Baum, M. Munowitz, A. N. Garroway, and A. Pines, Multiple quantum dynamics in solid state NMR, *J. Chem. Phys.* **83,** 2015–2025 (1985).
3. J. Baum and A. Pines, NMR studies of clustering in solids, *J. Am. Chem. Soc.* **108,** 7447–7454 (1986).
4. J. Baum, K. K. Gleason, A. Pines, A. N. Garroway, and J. A. Reimer, Multiple quantum NMR study of clustering in hydrogenated amorphous silicon, *Phys. Rev. Lett.* **56,** 1377–1380 (1986).
5. D. Suter, S. B. Liu, J. Baum, and A. Pines, Multiple quantum NMR excitation with a one-quantum Hamiltonian, *Chem. Phys.* **114,** 103–109 (1987).
6. M. A. Petrich, K. K. Gleason, and J. A. Reimer, Structure and properties of amorphous hydrogenated silicon carbide, *Phys. Rev. B* **36,** 9722–9731 (1987).
7. D. H. Levy and K. K. Gleason, Multiple quantum nuclear magnetic

resonance as a probe for the dimensionality of hydrogen in polycrystalline powders and diamond films, *J. Phys. Chem.* **96,** 8125–8131 (1992).

8. B. E. Scruggs and K. K. Gleason, Analysis of fluorocarbon plasma treated diamond powders by solid state ^{19}F nuclear magnetic resonance, *J. Phys. Chem.* **97,** 9187–9195 (1993).
9. S. J. Hwang, D. O. Uner, T. S. King, M. Pruski, and B. C. Gerstein, Characterization of silica catalyst supports by single and multiple quantum proton NMR spectroscopy, *J. Phys. Chem.* **99,** 3697–3703 (1995).
10. W. V. Gerasimowicz, A. N. Garroway, J. B. Miller, and L. C. Sander, Multiple quantum NMR studies of monomeric bonded silica phases, *J. Phys. Chem.* **96,** 3658–3661 (1992).
11. S. J. Limb, B. E. Scruggs, and K. K. Gleason, Distribution and motion of trifluoromethanesulfonate anions in poly(*p*-hydroxystyrene) and polystyrene films studied by multiple quantum NMR, *Macromolecules* **26,** 3750–3757 (1993).
12. B. E. Scruggs and K. K. Gleason, Photosensitive salt distribution in polymer films studied by ^{19}F multiple quantum NMR, *Macromolecules* **25,** 1864–1869 (1992).
13. G. Buntkowsky, E. Roessler, M. Taupitz, and H. M. Vieth, Adamantane as a probe for studies of spin clustering with multiple quantum NMR, *J. Phys. Chem A* **101,** 67–75 (1997).
14. J. G. Pearson, B. F. Chmelka, D. N. Shykind, and A. Pines, Multiple quantum NMR study of the distribution of benzene in NaY zeolite, *J. Phys. Chem.* **96,** 8517–8522 (1992).
15. M. Munowitz, A. Pines, and M. Mehring, Multiple quantum dynamics in NMR: A directed walk through Liouville space, *J. Chem. Phys.* **86,** 3172–3182 (1987).
16. E. B. Feldman and S. Lacelle, Multiple quantum nuclear magnetic resonance in one-dimensional quantum spin chains, *J. Chem. Phys.* **107,** 7067–7084 (1997).
17. G. G. Cho and J. P. Yesinowski, ^{1}H and ^{19}F multiple quantum NMR dynamics in quasi-one-dimensional spin clusters in apatites, *J. Phys. Chem.* **100,** 15716–15725 (1996).
18. S. Lacelle, S. J. Hwang, and B. C. Gerstein, Multiple quantum nuclear magnetic resonance of solids: A cautionary note for data analysis and interpretation, *J. Chem. Phys.* **99,** 8407–8413 (1993).
19. G. G. Cho and J. P. Yesinowski, Multiple quantum NMR dynamics in the quasi-one-dimensional distribution of protons in hydroxyapatite, *Chem. Phys. Lett.* **205,** 1–5 (1993).
20. M. Tomaselli, S. Hediger, D. Suter, and R. R. Ernst, Nuclear magnetic resonance polarization and coherence echoes in static and rotating solids, *J. Chem. Phys.* **105,** 10672–10681 (1996).
21. O. N. Antzutkin and R. Tycko, High-order multiple quantum excitation in ^{13}C nuclear magnetic resonance spectroscopy of organic solids, *J. Chem. Phys.* **110,** 2749–2752 (1999).
22. W. S. Warren, D. P. Weitekamp, and A. Pines, Theory of selective excitation of multiple quantum transitions, *J. Chem. Phys.* **73,** 2084–2099 (1980).
23. A. Messiah, "Quantum Mechanics," Vol. 2, Wiley, New York (1958).
24. D. P. Weitekamp, Time-domain multiple quantum NMR, *in* "Advances in Magnetic Resonance," Vol. 11, pp. 111–270, Academic Press, New York (1983).
25. V. Muñoz and L. Serrano, Development of the multiple sequence approximation within the AGADIR model of α-helix formation. Comparison with Zimm–Bragg and Lifson–Roig formalisms, *Biopolymers* **41,** 495–509 (1997).
26. A. E. Bennett, C. M. Rienstra, M. Auger, K. V. Lakshmi, and R. G. Griffin, Heteronuclear decoupling in rotating solids, *J. Chem. Phys.* **103,** 6951–6958 (1995).